Influence of molecular processes on the hydrogen atomic system in an expanding argon-hydrogen plasma

Influence of molecular processes on the hydrogen atomic system in an expanding argon–hydrogen plasma

R. F. G. Meulenbroeks, R. A. H. Engeln, C. Box, I. de Bari, M. C. M. van de Sanden, J. A. M. van der Mullen, and D. C. Schram
Eindhoven University of Technology, Department of Physics, P. O. Box 513 5600 MB Eindhoven, The Netherlands

(Received 30 August 1994; accepted 10 November 1994)

An expanding thermal arc plasma in argon–hydrogen is investigated by means of emission spectroscopy. The hydrogen can be added to the argon flow before it enters the thermal arc plasma source, or it can be flushed directly into the vacuum expansion vessel (1–20 vol % H_2). The atomic state distribution function for hydrogen, measured at a downstream distance of 20 mm, turns out to be very different in the two cases. For injection in the arc, three-particle recombination is a primary source of hydrogen excitation, whereas measurements with hydrogen injected into the vessel clearly point to a molecular channel (dissociative recombination of formed ArH^+) populating atomic hydrogen levels. © *1995 American Institute of Physics.*

I. INTRODUCTION

Expanding thermal arc plasmas are used in a variety of applications such as plasma deposition and etching and particle sources.[1–4] The fundamental study of this type of plasma has concentrated on pure argon plasmas and argon–hydrogen mixtures.[5–8] The plasma expands out of a cascaded arc through a conically shaped nozzle into a low-pressure background. The initially supersonic expansion ends in a stationary shock after 40–70 mm, which is followed by a subsonic relaxation region.

As was reported before,[7,8] hydrogen molecules play a major role in the very fast ionization loss that has been measured using Thomson scattering on an expanding argon–hydrogen plasma. Atomic processes cannot account for this anomalous loss of ions. It has been made plausible[8] that at least an important fraction of these hydrogen molecules must originate from the stainless steel vessel walls. The fact that the volume of the vessel (about 300 l) causes the residence time of particles to be fairly large (around 1 s) may induce a recirculation pattern inside the vessel. This flow could well be responsible for the transport of the formed molecules back into the plasma.[7]

The following set of reactions is responsible for the fast ionization loss:

$$\begin{aligned} &Ar^+ + H_2 \rightarrow ArH^+ + H, \\ &ArH^+ + e \rightarrow Ar + H^*. \end{aligned} \tag{1}$$

At temperatures in the expansion (around 0.2 eV), the competing charge exchange reaction (the creation of H_2^+) is of little importance.[9] If the formed ArH^+ ion carries little rovibrational energy, the excited hydrogen atom is formed in the $p=2$ state. If important rovibrational excitation is present (the potential well of the molecular ion has a depth of about 4 eV[10]), hydrogen states $p=3$ or higher may be formed, which can be readily observed by simple emission spectroscopy. The origin of the high rovibrational excitation of ArH^+ will be discussed later.

II. EXPERIMENT

The expanding plasma experiment has been described before,[5] and will only be summarized here. The thermal plasma source (a cascaded arc) is operated at the same settings as used in Refs. 7 and 8: arc current: 45 A, arc voltage 100–140 V (depending on the hydrogen seed fraction), background pressure 40 Pa, and total gas flow 3.5 standard liters per minute (SLM). The hydrogen seed fractions are 1,2,3,4,5,7,10, and 20 vol % H_2; hydrogen is added to the flow before it enters the cascaded arc or injected directly into the vessel. These two conditions will be referred to as "arc seeding" and "vessel injection," respectively.

The optical emission spectroscopy (OES) experiment has been described in Ref. 7. It contains a fairly standard mirror-scanned optical system. A few modifications have been implemented: a different monochromator (Bentham M300) with a Hamamatsu R1617 photomultiplier tube is used. The slit widths are chosen to obtain a resolution of 0.16 nm. Furthermore, an extra mirror was added to make possible the use of an external ribbon lamp for calibration of the last part of the optical system (including the last two lenses, the monochromator, and the photomultiplier, Fig. 1). The calibration procedure is the following. At the beginning of a measuring period of about four weeks, a calibration using a tungsten ribbon lamp, placed inside the vacuum vessel (at the plasma position), is performed. Immediately after that calibration (covering the entire light path) a calibration using the external ribbon lamp is made, covering the last part of the optical system. This is done by turning the step motor-driven rotating mirror (RM in Fig. 1) in order to focus the external ribbon lamp on the pinhole (Fig. 1). Every two or three days, this latter calibration is repeated, and the calibration with the ribbon lamp in the vessel is repeated at the end of the measuring period. The differences between the calibrations appear to be quite small (typically 3%).

This calibration procedure makes possible a very accurate determination of absolute level densities of atomic

 1070-664X/95/2(3)/1002/7/$6.00

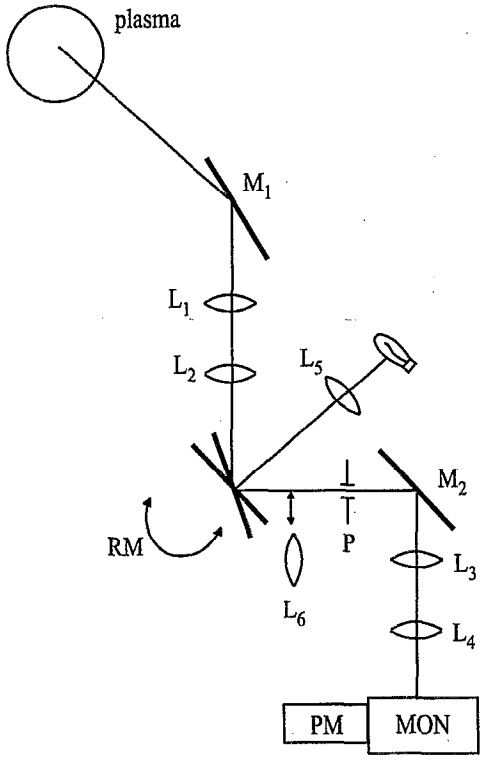

FIG. 1. The emission spectroscopy experiment. The plasma radiation is focused on the entrance slit of the monochromator (MON) by a system of lenses (L_1, $f=750$ mm; L_2, $f=500$ mm; L_3, $f=200$ mm; and L_4, $f=150$ mm) and mirrors (M_1,M_2). Here P designates a 0.5 mm diam pinhole and PM the photomultiplier tube. Photon counting electronics are used to record the incoming radiation. A rotating mirror (RM) is used to make lateral scans of the plasma. These are Abel inverted later to obtain radial profiles. An external ribbon lamp (RL) is used for day-to-day checks of the last part of the optical system. To do this, the rotating mirror has to be turned, and the ribbon is focused on the pinhole by lenses L_5 ($f=200$ mm) and L_6 ($f=150$ mm). The latter can be (reproducibly) inserted in the optical system when a calibration using the external ribbon lamp is required.

states. The main source of error for the hydrogen states is the plasma reproducibility (10%–15%). In the case of argon, the inaccuracies in the transition probabilities (around 25%–50%) become dominant.[7,11]

All lateral scans are performed at a downstream axial distance of $z=20$ mm. The expansion axis is labeled z, with the origin at the expansion nozzle. The lateral scans are converted into radial profiles by means of Abel inversion, yielding radial profiles of the absolute level density per statistical weight. Measurements are performed on the Balmer series of hydrogen (data can be found in Ref. 11 or 7), as well as on several argon lines (also given in Ref. 7). The latter was mainly done to check the calibration: in our recombining plasma jet, the population factors b_p (an indication of the departure from Saha equilibrium[7,12]) should tend to unity for highly excited levels. For a pure argon expanding plasma, one can use the measured values of T_e and n_e (Thomson scattering[5,7]) to calculate the b_p factors. In this case, a very satisfactory approach to unity is observed for levels near the continuum, where a Saha equilibrium is expected (compare

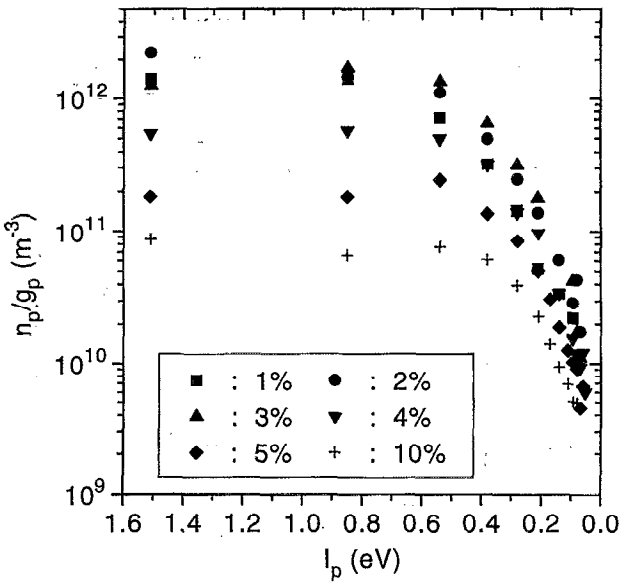

FIG. 2. The Boltzmann plots n_p/g_p vs I_p for the arc seeding case at a downstream distance of 20 mm, for different hydrogen seed fractions. The hydrogen is admixed to the flow before it enters the arc.

Ref. 7). This constitutes a reliable check of the calibration of the OES system, as the Thomson scattering data are known to be very accurate (compare Ref. 5).

III. RESULTS

The results will be discussed in two parts. For the sake of clarity, we shall first discuss the measurements where hydrogen is added to the flow before it enters the arc (arc seeding), after which we shall turn to the second set of measurements, where the hydrogen is injected in the vacuum vessel.

A. Arc seeding

Typical n_p/g_p vs I_p (absolute level densities per statistical weight versus the ionization energy of the level concerned) plots are given in Fig. 2. The character is clearly recombining. Sometimes a slight inversion is observed. Strong inversions can be observed in similar plasmas (e.g., Ref. 13, where a similar setup with a magnetic field is used).

To calculate the population factors b_p, we need the hydrogen ion concentration. For arc seeding, the ratio of argon to hydrogen ions can be calculated with the method described in Refs. 14 and 7, using highly excited hydrogen and argon levels. The n_e and T_e values needed for the calculation are taken from Ref. 8. The H^+/Ar^+ concentration ratios are similar to those reported in Ref. 7: around 1:70 for a 2 vol % seed fraction, increasing to 1:4 for 3 vol %. For measurements with higher seed fractions (above 4 vol %), the ratio cannot be determined, because the argon emission disappears. This is a result from the arc ionization changing from argon to hydrogen. The lines used for the H^+/Ar^+ ratio calculation are hydrogen 377.1 and 388.9 nm, and argon 531.8 and 506.0 nm (see Refs. 7 and 11), as these levels should be well within the region of Saha equilibrium.

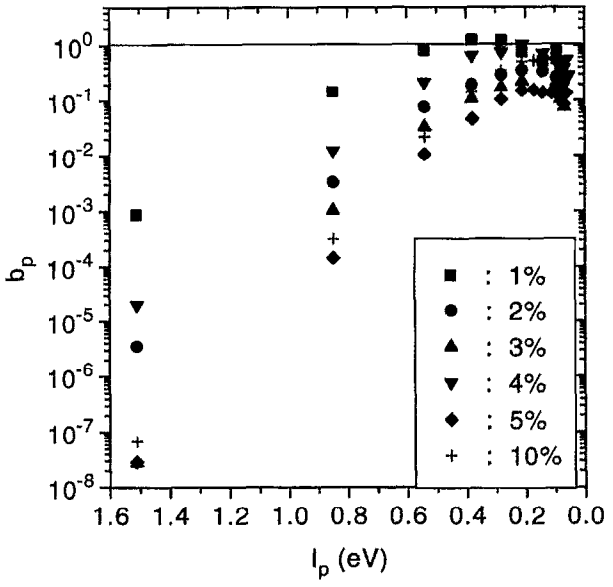

FIG. 3. The population factors b_p vs I_p for the arc seeding case at a downstream distance of 20 mm.

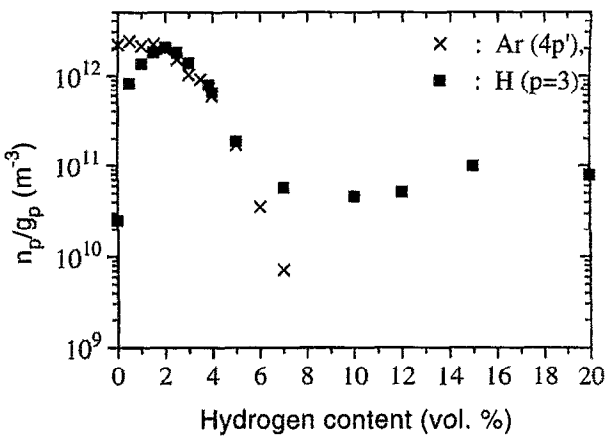

FIG. 4. The hydrogen $p=3$ and argon $4p'$ level densities per statistical weight versus the hydrogen arc seed fraction for the arc seeding case. The argon n_p/g_p values have been divided by 20 to make clear the difference in behavior.

Figure 3, then, gives the b_p vs I_p plots, for arc seed fractions of 1–10 vol %. The absolute b_p values cannot be considered very accurate for higher seed fractions, where the ion concentration ratios are unknown. The "bulge" in b_p that was reported before Ref. 7 around level $p=5-7$ is not observed in all cases. It should be noted that the deviation from equilibrium (e.g., by comparing the b_p values for $p=3$) becomes larger for higher seed fractions: this is consistent with the observed decrease in n_e, as reported in Ref. 8. Clearly, the electron impact processes lose importance for higher seed fractions, causing the lower part of the excitation system to become more and more radiation dominated.

We can try to explain the observed hydrogen population densities by considering only three-particle recombination of H^+. To do so, we have to determine which part of the total deexcitation (three-particle recombination) flow passes a certain level, say $p=3$. At ambient conditions (n_e around 2.5×10^{19} m^{-3} and T_e around 1500 K), the hydrogen system is dominated by radiative deexcitation below level $p=4$. Above that level, collisional deexcitation is dominant, resulting in mainly stepwise deexcitation in that part of the system.[12] Radiative deexcitation being dominant in the lower part of the excitation system, a comparison of the radiative transition probabilities[11] starting from $p=4$ shows that about one-third of the recombination flow should pass $p=3$.

The rate constant for three-particle recombination is taken from Van de Sanden:[15] $K_{3p}=3.3\times10^{-21}n_+n_e^2\,T_e^{-4.5}$ $m^6\,s^{-1}$. As stated above, we assume the depopulation of $p=3$ to be due to radiation: the collisional deexcitation process can be shown to be slower by a factor of about 10. Thus, the total $p=3$ density $H_{p=3}$ can be calculated:

$$n_{\mathrm{H},p=3}\cdot A_{3,\mathrm{downward}}\approx\tfrac{1}{3}n_e^2\cdot n_{\mathrm{H}^+}\cdot K_{3p}, \tag{2}$$

with $A_{3,\mathrm{downward}}$ the total radiative destruction of the level (10^8 s^{-1}). For $n_e=3.4\times10^{19}$ m^{-3}, $T_e=1500$ K, and an $n_{H^+}:n_{Ar^+}$ ratio of 1:70, this results in $n_e/g_3\approx2\times10^{12}$ m^{-3}. This estimate is in agreement with the observed 2.5×10^{12} m^{-3} for a 2% arc seed fraction. No additional processes need to be considered to explain the hydrogen level population at the center of the plasma jet. At the edges, some extra input may be necessary to explain the observed population of hydrogen levels, as the electron density profile is more narrow than the hydrogen $p=3$ density profile, while the electron temperature profile is relatively flat. This means that three-particle recombination can no longer fully account for the observed emission at the edges of the plasma jet.

An interesting feature is observed when measurements are performed at H_α and argon 696.5 nm ($4p'$) for increasing hydrogen seed fractions; see Fig. 4. For argon, a steady decrease is observed, caused by the arc ionization changing from argon to hydrogen. Here H_α shows a behavior similar to that reported in Ref. 8. The H_α radiation (above 7 vol %) can probably be attributed to three-particle recombination, as no argon ions are left.[8] An extra input, however, could be formed by dissociative recombination of H_2^+ ions formed by charge exchange between H^+ and rovibrationally excited H_2 molecules.[4] To end in $p=3$, the participating H_2 molecule should carry considerable rovibrational excitation (3–4 eV). For lower seed fractions, where Ar^+ is the most abundant ion, reactions (1) probably are dominant, as the H_2 molecule does not need to carry that much rovibrational excitation to make a creation of the $p=3$ state possible.

If we assume, for the arc seeding case, three-particle recombination to be dominant, the strong increase in H_α for low seed fractions should be caused by more and more hydrogen entering the arc. The decrease above 2 vol % must then be caused by the arc becoming less efficient, as indicated by Thomson scattering measurements.[8]

B. Vessel injection

In the case of vessel injection, the hydrogen is injected far away from the expansion nozzle in the vessel itself. The flows are kept the same as in the arc seeding case. It is useful to point to the main differences between arc seeding and vessel injection.

(a) When hydrogen is injected into to vacuum vessel, we can be sure that our plasma source remains unaffected: the cascaded arc will produce a pure argon plasma, which constitutes a well-known source of argon ions.[5,15] On the other hand, other measurements have learned that the arc plasma source changes when hydrogen is mixed to the argon flow before it enters the arc; a lower electron density when H_2 is injected in the arc.[8]

(b) A possible difference concerns the rovibrational population of the hydrogen molecules inside the vessel. When hydrogen is injected in the vessel at 300 K, only the $v=0$ vibrational state is populated. As the plasma itself has a temperature of only 0.2 eV, any significant rovibrational excitation (e.g., 2 eV or more) should come from wall association.[16] This process could bring about a "second generation" of hydrogen molecules formed by the association of hydrogen atoms [originating from reactions (1)] at the vessel walls. When hydrogen is injected in the arc, some rovibrational excitation may originate from molecules surviving the arc (where the temperatures are around 1 eV). It is, however, more probable that excited hydrogen molecules are formed at the vessel walls, as has been concluded before.[1,7,8]

(c) For the OES work, the main difference lies in the population mechanism of the hydrogen excited levels. As was shown above, three-particle recombination can fully account for the observed $p=3$ population for the arc seeding case. The fact that the population factors b_p approach unity for low I_p also points in this direction. When hydrogen is injected in the vessel, only one channel of hydrogen excited level population is still possible: dissociative recombination of rovibrationally excited ArH^+ ions ending in H excited states. It should be pointed out that no H^+ or excited H can be formed by electron impact in view of an extremely small Boltzmann exponent at ambient temperatures of 0.2 eV. In the following, it will be shown that a relatively small amount of rovibrationally excited molecular ions suffices to account for the observed hydrogen Balmer radiation in the vessel injection case.

Figure 5 gives the n_p/g_p vs I_p plots for the vessel injection case. The distribution is clearly different from the arc seeding case: only the lower three to five levels are observed. Since these levels are not expected to be in Saha equilibrium with the continuum, a calculation of ion concentration ratios (as discussed in Sec. III A) is probably not possible. Also, b_p factors cannot be calculated. Furthermore, the H^+ concentration must be very low, since a significant hydrogen ion concentration should bring about emission of higher excited states, populated by three-particle recombination.

Before turning to a more quantitative explanation of these results, we must exclude one specific excitation mechanism for $p=3$: dissociative recombination of (low excited) ArH^+ ending in $p=2$ and subsequent collisional excitation to $p=3$. We can get an estimate of the rate constant $K_{2,3}$ for

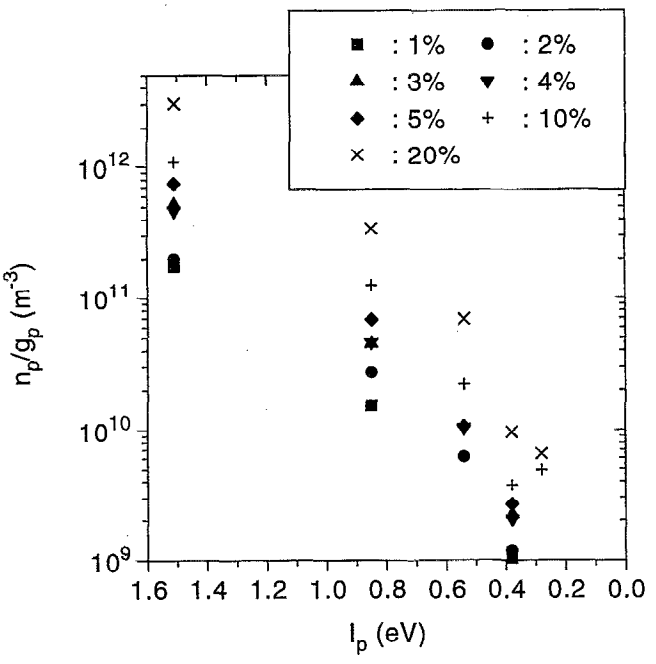

FIG. 5. The Boltzmann plots (n_p/g_p vs I_p) for different hydrogen seed fractions, when hydrogen is injected into the vessel. Note the very pronounced difference with Fig. 2, due to different excitation mechanisms in the two cases.

this excitation process by applying a hard-sphere approximation:[12]

$$K_{n,n+1} \approx 4\pi a_0^2 \cdot p^4 \cdot v_{\text{th}} \frac{g_{n+1}}{g_n} \exp\left(\frac{-\Delta E_{n,n+1}}{kT_e}\right), \tag{3}$$

where a_0 is Bohr's radius, p is the principal quantum number, g_n is the statistical weight of level p, v_{th} is the electron thermal speed, $\Delta E_{n,n+1}$ is the energy gap between levels p and $n+1$, and k is Boltzmann's constant. For the ambient conditions ($n_e=5.2\times10^{19}$ m^{-3}, $T_e=2000$ K), Eq. (3) yields $K_{2,3}\approx3.3\times10^{-17}$ $m^3\,s^{-1}$. If the population of level $p=3$ is governed by a Corona-like balance of electron excitation from $p=2$ and radiative destruction, we can write

$$n_{\text{H},p=3} \cdot A_{3,\text{downward}} = n_{\text{H},p=2} \cdot n_e \cdot K_{2,3}, \tag{4}$$

which for a 2 vol % would lead to a total $p=2$ density of 2.1×10^{17} m^{-3}. If these $p=2$ states are produced by dissociative recombination of ArH^+, the following balance should hold (the plasma is optically thin for hydrogen radiation in the case of low hydrogen concentrations):

$$n_{\text{H},p=2} \cdot A_{2,1} = n_{\text{Ar}^+} \cdot n_{\text{H}_2} \cdot K_1, \tag{5}$$

where the rate constant K_1 for the formation of ArH^+ is 1.1×10^{-15} $m^3\,s^{-1}$ (Ref. 17) at ambient temperatures. The transition probability $A_{2,1}=4.7\times10^8$ s^{-1}. The second dissociative recombination step of reactions (1) is known to be

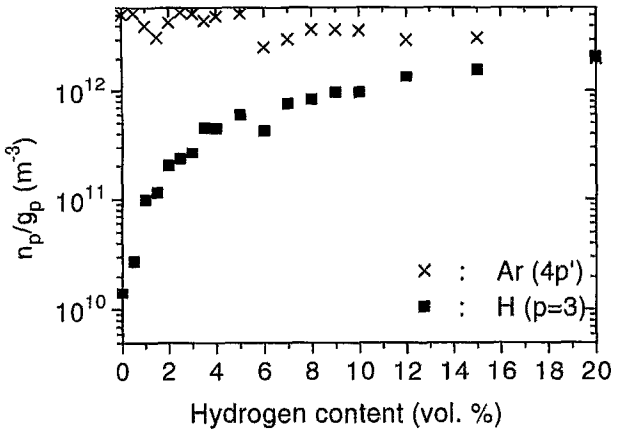

FIG. 6. The hydrogen $p=3$ and argon $4p'$ level densities per statistical weight versus the hydrogen admixture: hydrogen is injected in the vessel. The argon $4p'$ densities have been divided by a factor 8 to make possible a comparison of the behavior of the two excited states.

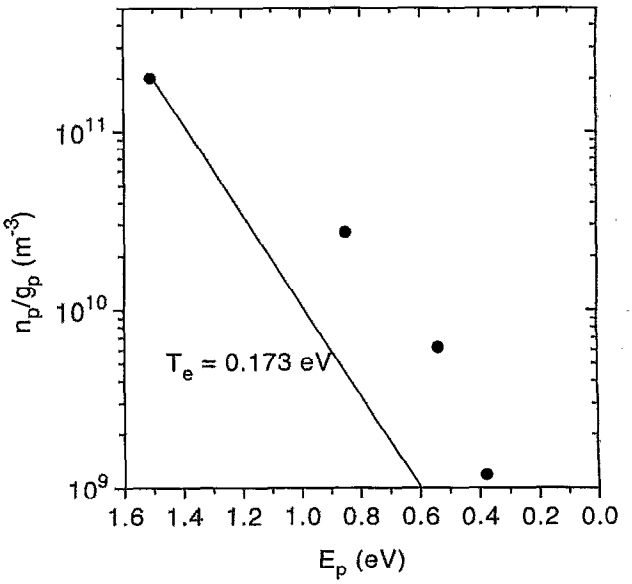

FIG. 7. A Boltzmann plot for 2 vol % hydrogen injection in the vessel. To indicate the possible Boltzmann equilibrium starting from level $p=3$, a line designating the (Thomson scattering) value of T_e has been drawn.

faster by a factor of about 100, depending on conditions. As the first step thus limits the production of ArH^+ ions, we have to use K_1 in the above balance. Equation (5) leads to a H_2 density of about 1.7×10^{21} m^{-3}. This value is unrealistic, as the total neutral density at $z=20$ mm is around 9×10^{20} m^{-3}.[8]

For the vessel injection case, we can thus safely exclude the following population mechanisms for $p=3$ and higher: (a) three-particle recombination (which would require a significant H^+ density), (b) electron excitation (the Boltzmann exponent is extremely small), and (c) dissociative recombination of ArH^+ ending on $p=2$ and subsequent collisional excitation to $p=3$ (which would require an unrealistic H_2 density).

In our view, only one mechanism remains: dissociative recombination of rovibrationally excited ArH^+. We can estimate the amount of hydrogen needed to accomplish the observed hydrogen excited level populations. We neglect for the moment the question of whether a rovibrationally excited hydrogen molecule that participates in reaction (1) actually produces a rovibrationally excited ArH^+ ion. We shall come back to this later. A balance analogous to Eq. (5) can be written for $p=3$:

$$n_{H,p=3}\cdot A_{3,\text{downward}} = n_{Ar^+}\cdot n_{H_2^{v,J}}\cdot K_1 . \tag{6}$$

In this balance, we know the electron density ($n_e=5.2\times10^{19}$ m^{-3}), which is equal to the argon ion density in the vessel injection case. Inserting the known values in Eq. (6) yields a density of rovibrationally excited molecules (with enough internal energy to make possible the excitation of the ArH^+ ion and, thus, of the formed H atom) of $n_{H_2^{v,J}} = 6.3\times10^{15}$ m^{-3} for a 2 vol % injection in the vessel. If we assume the maximum total H_2 density in the plasma to be equal to 2% of the total neutral density (9×10^{20} m^{-3}), the H_2 density would amount up to 1.8×10^{19} m^{-3}. If any rovibrational excitation is supplied by wall association, the number of excited hydrogen molecules appears to be reasonable.

Support for this production mechanism for $p=3$ states can also be deduced from Fig. 6, which shows the behavior of H $p=3$ and argon $4p'$ densities for different vessel seed fractions. Equation (6) predicts the $p=3$ density to be proportional to the $H_2^{v,J}$ density (for a constant Ar^+ density). Figure 6 shows, that the $p=3$ population is proportional to the *total* H_2 density. That the Ar^+ density must be more or less constant is indicated by the fact that the argon $4p'$ level density decreases only by a factor of 2–3 (the argon population is dominated by three-particle recombination). A logarithmic representation is chosen for Fig. 6 (even though it obscures the mentioned proportionality) to clearly represent the lower $p=3$ data.

To illustrate the effect, that the population of $p=3$ alone is not sufficient to explain the measurements, Fig. 7 gives the n_p/g_p values for a 2 vol % vessel injection. The drawn line represents a Boltzmann line with the electron temperature. Electron collisions are clearly not energetic enough to explain the population of higher excited levels, as the latter are consequently above the Boltzmann line. Thus, some extra input at these higher levels (up to $p=5$) has to be made plausible. In the following, we shall show that this is indeed possible if the H_2 molecules that participate in reaction (1) carry considerable rovibrational excitation.

Thus we return to the question of whether a rovibrationally excited hydrogen molecule actually produces a rovibrationally excited ArH^+ ion. Following Gislason *et al.*,[18] a simple argument can be constructed. As the first reaction in

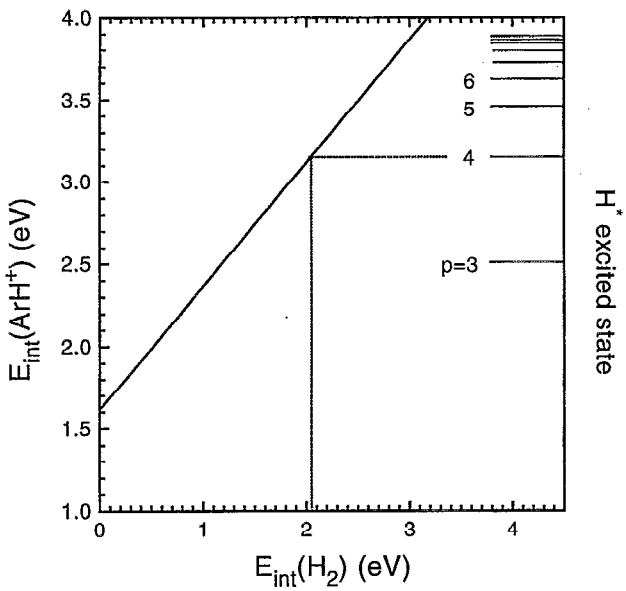

FIG. 8. The relation between the internal energies (E_{int}) of H_2 and ArH^+ during the first reaction of Eq. (1). The H* excited levels that can (energetically) be reached during the subsequent dissociative recombination of ArH^+ are indicated. For example, to reach $p=4$, the H_2 molecule has to be rovibrationally excited by about 2 eV. The assumption is that half of the vibrational energy is kinetic at the instant of reaction.

Eq. (1) is a classic spectator stripping reaction, it can be thought to be instantaneous. The transferral of internal energy from $H_2(v,J)$ to $ArH^+(v',J')$ then depends on the amount of vibrational energy that is potential energy at the instant of reaction. This leads to the following estimate for the internal energy of the formed ArH^+:

$$E_{int}(ArH^+) \approx \tfrac{1}{2}E + \tfrac{3}{4}E_{int}(H_2) - \Delta H_0^0, \qquad (7)$$

where E represents the relative kinetic energy of the reactants, $E_{int}(X)$ is the internal energy of species X, and ΔH_0^0 is the reaction enthalpy (equal to -1.53 eV). It is assumed, that half the vibrational energy is kinetic at the instant of reaction.

If we represent Eq. (7) in a figure, Fig. 8 is obtained. It shows the relation between the internal energy of the H_2 molecule and the internal energy of the ArH^+ molecular ion. If a (wall-associated) H_2 molecule carries a large amount of rovibrational excitation, highly excited levels can be formed in the dissociative recombination of ArH^+. This mechanism can explain the observed population of excited states.

IV. CONCLUSIONS

The investigation of the argon–hydrogen plasma jet by OES and Thomson scattering leads to the following conclusions.

When hydrogen is mixed to the flow before it enters the cascaded arc, the hydrogen emission in the expanding plasma can be explained by three-particle recombination at the center of the plasma jet at $z=20$ mm. If there is any input from dissociative recombination, it must be at least an order of magnitude less important at the center. It may, however, be of importance at the plasma periphery. The importance of three-particle recombination at the plasma center is confirmed by comparing the $p=3$ densities for the arc seeding and vessel injection cases: at a 2 vol % seed fraction, the latter are lower by a factor of 10. Higher seed fractions cannot be easily compared, as the arc efficiency is going down for the arc seeding case. A possible extra input for higher seed fractions could be formed by dissociative recombination of H_2^+ ions.

The population factors b_p approach unity for low I_p, pointing to some kind of Saha equilibrium close to the continuum (arc seeding case). The "bulge" in the hydrogen b_p's does not occur for all seed fractions and depends critically on the determination of n_e and the Ar^+/H^+ ratio.

For the arc seeding case it is clear that the arc ionization changes from Ar^+ to H^+, as all argon emission disappears for higher seed fractions. The efficiency of the arc seems to decrease as well, as indicated by the H_α intensity behavior for different seed fractions.

When hydrogen is injected in the vessel, only one possible excitation mechanism remains: dissociative recombination of rovibrationally excited ArH^+, ending on $p=3$ or even higher. A Boltzmann equilibrium from this level upward cannot fully account for the population of the higher excited levels ($p=4-6$). An extra input therefore has to be assumed at these levels. This requires the ArH^+ to carry considerable rovibrational excitation. In a simple argument, this excitation could be produced by associative charge exchange with rovibrationally excited H_2 molecules, produced at the vessel walls.

ACKNOWLEDGMENTS

The authors would like to thank H. M. M. de Jong and M. J. F. van de Sande for their skillful technical assistance and M. N. A. Beurskens for the Thomson scattering measurements.

This work is supported by the Netherlands Technology Foundation (STW). The work of M. C. M. van de Sanden is supported by the Royal Netherlands Academy of Arts and Sciences (KNAW).

[1] R. F. G. Meulenbroeks, D. C. Schram, L. J. M. Jaegers, and M. C. M. van de Sanden, Phys. Rev. Lett. **69**, 1379 (1992).
[2] A. J. M. Buuron, G. J. Meeusen, J. J. Beulens, M. C. M. van de Sanden, and D. C. Schram, J. Nucl. Mat. **200**, 430 (1993).
[3] A. T. M. Wilbers, G. J. Meeusen, M. Haverlag, G. M. W. Kroesen, and D. C. Schram, Thin Solid Films **204**, 59 (1991).
[4] M. J. de Graaf, R. Severens, R. P. Dahiya, M. C. M. van de Sanden, and D. C. Schram, Phys. Rev. E **48**, 2098 (1993).
[5] M. C. M. van de Sanden, J. M. de Regt, G. M. Janssen, J. A. M. van der Mullen, D. C. Schram, and B. van der Sijde, Rev. Sci. Instrum. **63**, 3369 (1992).
[6] R. F. G. Meulenbroeks, P. A. A. van der Heyden, M. C. M. van de Sanden, and D. C. Schram, J. Appl. Phys. **75**, 2775 (1994).
[7] R. F. G. Meulenbroeks, A. J. van Beek, A. J. G. van Helvoort, M. C. M. van de Sanden, and D. C. Schram, Phys. Rev. E **49**, 4397 (1994).
[8] R. F. G. Meulenbroeks, R. A. H. Engeln, M. N. A. Beurskens, R. M. J. Paffen, M. C. M. van de Sanden, J. A. M. van der Mullen, and D. C. Schram, "Argon–hydrogen expanding plasma jet: Model and experiments," accepted for publication in Plasma Sources Sci. Technol.
[9] E. A. Gislason and G. Parlant, J. Chem. Phys. **94**, 6598 (1991).

[10]D. M. Hirst, M. F. Guest, and A. P. Rendell, Mol. Phys. **77**, 279 (1992).
[11]W. L. Wiese, M. W. Smith, and B. M. Miles, *Atomic Transition Probabilities* (National Bureau of Standards, Washington, DC, 1969), Monograph No. NSRDS-NBS22.
[12]J. A. M. van der Mullen, Phys. Rep. **191**, 109 (1991).
[13]H. Akatsuka and M. Suzuki. Phys. Rev. E **49**, 1534 (1994).
[14]G. J. Meeusen, E. A. Ershov-Pavlov, R. F. G. Meulenbroeks, M. C. M. van de Sanden, and D. C. Schram, J. Appl. Phys. **71**, 4156 (1992).
[15]M. C. M. van de Sanden, J. M. de Regt, and D. C. Schram, Phys. Rev. E **47**, 2792 (1993).
[16]B. Jackson and M. Persson, J. Chem. Phys. **96**, 2378 (1992).
[17]K. M. Ervin and P. B. Armentrout, J. Chem. Phys. **83**, 166 (1985).
[18]E. A. Gislason (private communication, 1994); K. Dong, E. A. Gislason, and M. Sizun, Chem. Phys. **179**, 143 (1994).